

PNAS

www.pnas.org

Supplementary Information for

Genetically and culturally diverse botanical hypotensive folk medicines share a unifying molecular mechanism: KCNQ5 activation

Rían W. Manville, Jennifer van der Horst, Kaitlyn E. Redford, Benjamin B. Katz, Thomas A. Jepps and Geoffrey W. Abbott

Corresponding authors: Drs. Geoffrey W. Abbott (abbottg@uci.edu) and Rían W. Manville (rmanvill@uci.edu)

This PDF file includes:

Supplementary text – photo attributions

Supplementary Materials and Methods

Supplementary References

Figures S1 to S8

Tables S1 to S15

Supplementary Text

Photo attributions

Figure 1D and Figure S2A

Thyme, Oregano, Basil, Curly parsley, Italian parsley, Wheatgrass: Photos taken by GWA

Lavender, Ginger rhizome: Photos taken by Bo Abbott

Spearmint

https://commons.wikimedia.org/wiki/File:Mentha_spicata_02.jpg

https://commons.wikimedia.org/wiki/Commons:GNU_Free_Documentation_License,_version_1.2

Marjoram

https://commons.wikimedia.org/wiki/Origanum_majorana#/media/File:Origanum_majorana_002.JPG

<https://creativecommons.org/licenses/by-sa/3.0/>

Chamomile

[https://en.wikipedia.org/wiki/Chamomile#/media/File:Kamomillaunion_\(Matricaria_recutita\).JPG](https://en.wikipedia.org/wiki/Chamomile#/media/File:Kamomillaunion_(Matricaria_recutita).JPG)

<https://creativecommons.org/licenses/by-sa/3.0/deed.en>

Tarragon

<https://www.publicdomainpictures.net/en/view-image.php?image=109577&picture=tarragon-leaves>

<https://creativecommons.org/publicdomain/zero/1.0/>

Fennel seed

https://en.wikipedia.org/wiki/Fennel#/media/File:Fennel_seed.jpg

<https://creativecommons.org/licenses/by-sa/3.0/>

Sophora flavescens

https://commons.wikimedia.org/wiki/File:Sophora_flavescens.jpg

Sophora tonkinensis

<https://www.innerpath.com.au/matmed/herbs/Sophora-tonkinensis.htm>

Lemon grass

https://en.wikipedia.org/wiki/Cymbopogon#/media/File:YosriNov04Pokok_Serai.JPG

<https://creativecommons.org/licenses/by/2.0/>

Figure 3a

Sophora flavescens root slices

Photo taken by Bo Abbott

Supplementary Materials and Methods

Preparation of plant extracts

Certified organic fresh basil (*Ocimum basilicum*), spearmint (*Mentha spicata*), marjoram (*Oreganum marjorana*), oregano (*Origanum vulgare*), tarragon (*Artemisia dracuncululus*) and thyme (*Thymus vulgaris*), each grown at Jacobs Farm (Pescadero, CA, US), certified organic dried, powdered Frontier Co-op (Norway, IA, US) ginger root (*Zingiber officinale*) and whole fennel seed (*Foeniculum vulgare*), organic curly parsley (*Petroselinium crispum*), Italian parsley (*Petroselinium crispum neopolitanum*) and wheatgrass (*Triticum aestivum*) were sourced from Mother's Market and Kitchen (Irvine, CA, US). Chamomile flowers (*Matricaria chamomilla*) were sourced from Grateful Desert (Joshua Tree, CA, US). Fresh lavender (*Lavandula angustifolia*) was collected in August 2018 from the garden of the senior author (GWA). Fresh herbs, chamomile flowers, fennel seeds and dried ginger root were homogenized using a blender (SharkNinja, Needham, MA, US). Flat discs of GMP-certified, Chinese Pharmacopeia Grade You Ji Ku Shen (*Sophora flavescens* root) (Nuherbs, San Leandro, CA, US) and Shan Dou Gen (Vietnamese Sophora root and rhizome) (*Sophora tonkinensis*) in concentrated granule form (Guangdong Yifang Pharmaceutical Corporation, Foshan City, China) were homogenized with a bead mill in 50 ml tubes using porcelain beads (Omni International, Kennesaw, GA, US).

We performed methanolic extractions (80% methanol/20% water) of all 15 botanical homogenates for 48 hours at room temperature with occasional inversion of the bottles to resuspend the extract. Following this, the extracts were filtered using Whatman filter paper #1 (Whatman, Maidstone, UK) and then the methanol was removed by evaporation either in a fume hood for 16-48 hours at room temperature or using a rotary evaporator (Cole-Parmer, Vernon Hills, IL, US). The extracts were next centrifuged for 10 minutes at 15 °C, 4000 RCF to remove remaining particulate matter and then stored at -20 °C. On the day of electrophysiological recording, the extracts were thawed and then diluted 1:100 in bath solution (see below) immediately before use.

Channel subunit cRNA preparation and *Xenopus laevis* oocyte injection

We generated cRNA transcripts encoding human KCNE1, KCNE3, KCNQ1, KCNQ2, KCNQ3, KCNQ4, KCNQ3*, KCNQ5, KCNQ5-SYG or KCNQ5-R212A by *in vitro* transcription using the T7 polymerase mMessage mMachine kit (Thermo Fisher Scientific), after vector linearization, from cDNA sub-cloned into plasmids incorporating *Xenopus laevis* β -globin 5' and 3' UTRs flanking the coding region to enhance translation and cRNA stability. We quantified cRNA by spectrophotometry. We generated mutant KCNQ5 cDNAs by site-directed mutagenesis with a QuikChange kit (Stratagene, San Diego, CA) and prepared the cRNAs as above. We injected defolliculated stage V and VI *Xenopus laevis* oocytes (Ecocyte Bioscience, Austin, TX and Xenocyte, Dexter, MI, US) with KCNE and/or KCNQ cRNAs (5-20 ng). We incubated the oocytes at 16 °C in Barth's saline solution (Ecocyte) containing penicillin and streptomycin, with daily washing, for 3-5 days prior to two-electrode voltage-clamp (TEVC) recording.

Two-electrode voltage clamp (TEVC)

We performed TEVC at room temperature using a OC-725C amplifier (Warner Instruments, Hamden, CT) and pClamp10 software (Molecular Devices, Sunnyvale, CA) 3-5 days after cRNA injection as described in the section above. For recording, we placed the oocytes in a small-volume oocyte bath (Warner) and viewed them with a dissection microscope. We sourced

chemicals from Sigma unless otherwise stated. Bath solution was (in mM): 96 NaCl, 4 KCl, 1 MgCl₂, 1 CaCl₂, 10 HEPES (pH 7.6). We introduced aloperine, matrine, oxymatrine or the 1% plant extracts into the oocyte recording bath by gravity perfusion at a constant flow of 1 ml per minute for 3 minutes prior to recording. Pipettes were of 1-2 MΩ resistance when filled with 3 M KCl. We recorded currents in response to voltage pulses between -120 or -80 mV and +40 mV at 20 mV intervals from a holding potential of -80 mV, to yield current-voltage relationships, current magnitude, and for quantifying activation rate. Electrophysiology data analysis was performed with Clampfit (Molecular Devices) and Graphpad Prism software (GraphPad, San Diego, CA, USA); values are stated as mean ± SEM. Raw or normalized tail currents were plotted versus prepulse voltage and fitted with a single Boltzmann function:

Eq. 1

$$g = \frac{(A_1 - A_2)}{\left\{ 1 + \exp \left[\frac{(V_{1/2} - V)}{V_s} \right] \right\}} y + A_2$$

where g is the normalized tail conductance, A_1 is the initial value at $-\infty$, A_2 is the final value at $+\infty$, $V_{1/2}$ is the half-maximal voltage of activation and V_s the slope factor. We fitted activation and deactivation kinetics with single exponential functions.

Gas chromatography-mass spectrometry

To confirm the presence of aloperine in the specific *S. flavescens* extract that we used in our electrophysiological experiments, we first performed gas chromatography-mass spectrometry (GC-MS). *Sophora flavescens* extract in water was mixed in a 3:1 ratio with dichloromethane, centrifuged, and the dichloromethane layer was isolated for analysis.

Aloperine (Cayman Chemical Company, Ann Arbor, MI) was first dissolved fresh in methanol for GC/MS analysis (Fig. S3A). However, since the product information from Cayman indicates that aloperine is not stable in water for more than 1 day, the standard was next added to water, then extracted into dichloromethane to determine what new peaks are formed (Fig. S3B). The aloperine standard was dissolved in methanol (50mM) and diluted 1:1000 in water, which was then extracted using dichloromethane. GC-MS was performed using a Thermo Trace 1300 GC ISQ QD single quadrupole mass spectrometer. A 27-minute protocol starting at 40°C, increasing 10°C/minute to a final temperature of 290°C using a 25m DB5 column. The mass spectrometry data were acquired from 50-650 amu with a 0.2 second scan time. The data were analyzed using Chromeleon software. The *S. flavescens* extract was originally extracted into water (following methanol evaporation) and then functionally screened in aqueous buffer, therefore we compared it to the aloperine standard extracted from water (Fig, S3B). Comparison of the GC/MS chromatogram and extracted mass spectra indicated that the *S. flavescens* extract did contain masses similar to the aloperine standard at the expected elution times (Fig. S3C, D). This confirmed presence of aloperine in the *S. flavescens* extract we used for functional analysis.

Liquid chromatography-mass spectrometry

We next analyzed aloperine standards and dilutions of the *S. flavescens* extract using liquid chromatography-mass spectrometry (LC/MS), along with 2 μM aloperine added to *S. flavescens* extract for relative quantification. Since the aloperine changes/degrades in water, the common 233 Da base mass was tracked for single ion recording measurements. Extracted ion chromatograms for the 233 Da mass are shown in Fig. S4A-C. In the *S. flavescens* extract,

two peaks are seen, while the first peak only changes in intensity as the standard is added. This indicates that the first peak in the extract is more closely related to the aloperine standard spiked into water. While the second peak contains masses related to aloperine, its elution time indicates that it is different from the aloperine standard purchased from Cayman. A standard curve was produced using a range of aloperine standard solutions, which allowed for relative quantification of the aloperine in the extract, giving a value of $4.71 \pm 0.21 \mu\text{M}$ ($n = 4$) (Fig. S4D, E). This value is a conservative, calculated minimum content for aloperine in the original extract, since aloperine changes/degrades over time in water, and also given that the second peak may reflect, e.g., aloperine breakdown products. Thus, for the 1% extract applied to oocytes, the aloperine content was at minimum 47.1 nM, and was in actuality likely higher.

All samples and standards were prepared in a 10% acetonitrile, 90% water buffer. LC-MS was performed on a Waters Acquity H-class UPLC with a QDa mass analyzer and a photodiode array detector. The samples were run with a 105-600 Da mass range in positive mode for 5 minutes, with a sampling frequency of 2 Hz. The mobile phases buffers consisted of buffer B, 100% acetonitrile, and buffer A, 0.1% formic acid in water. A 5-minute gradient on an Acquity CSH C18 1.7 μm , 2.1x50mm column was run; starting at 3% B held for 0.75 minutes isocratic; after which, it ramped to 97% B over 3 minutes and held for 0.5 minutes at 97%B, finishing with a wash out back to 3% A at a constant flow rate of 0.3 mL/minute. Data analysis was performed using MassLynx software. Peaks corresponding to the molecular weight, M+H, of aloperine, 233 +/- 1 Da, were measured by integrating the area underneath and the concentration determined using the standard curve.

Radioligand binding competition assays

We placed each group of oocytes in a round-bottomed, 10-ml culture tube, washed them with ND96, and then resuspended them in ND96 containing 1 μM γ -[2,3- ^3H (N)]-aminobutyric acid (^3H -GABA) (Perkin Elmer, Waltham, MA) at 25-40 Ci/mMol specific activity, for a 30 minute incubation at room temperature, alone or with aloperine (100 μM or 1mM). We then washed oocytes washed four times in 16 °C ND96, transferred to individual wells in a 96 well plate and then lysed in 0.2% SDS in ND96. We transferred beach oocyte lysate to a scintillation vial containing 5 ml Cytoscint scintillation cocktail fluid (MP Biomedicals, Santa Ana, CA). We capped the vials, shook them, and then left them at room temperature for at least 30 min before scintillation counting in a Beckmann Coulter LS6500 liquid scintillation counter.

Mesenteric artery myography

Male wistar rats (13-14 weeks old) were killed by cervical dislocation before the intestines were removed and third-order mesenteric arteries dissected in ice-cold physiological saline solution (PSS), containing (in mM): 121 NaCl, 2.8 KCl, 1.6 CaCl₂, 25 NaHCO₃, 1.2 KH₂HPO₄, 1.2 MgSO₄, 0.03 EDTA and 5.5 glucose. Arterial segments, 2 mm in length, were mounted on 40 μm stainless-steel wires in a wire myograph (Danish Myo Technology, Aarhus, Denmark) containing PSS maintained at 37 °C and aerated with 95 % O₂ / 5 % CO₂. Changes in tension were recorded continuously by PowerLab and Chart software (ADInstruments, Oxford, U.K.). The arteries equilibrated at 37 °C before undergoing a passive force normalisation procedure (1). In the absence or presence of linopirdine (3 or 50 μM) (Sigma; Copenhagen, Denmark), segments of mesenteric artery were precontracted with 10 μM methoxamine before aloperine (Sigma; Copenhagen, Denmark) was applied at increasing concentrations from 0.3-300 μM . Statistical analysis was performed in Prism (version 8.0.2). A one-way ANOVA followed by a Sidak's multiple comparisons test was used to compare the logEC₅₀ values.

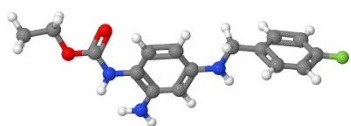
Chemical structures and *silico* docking

We plotted and viewed aloperine chemical structure and electrostatic surface potentials using Jmol, an open-source Java viewer for chemical structures in 3D: <http://jmol.org/>. For docking, we first altered the *Xenopus laevis* KCNQ1 cryoEM structure (2) to incorporate KCNQ3/KCNQ5 residues known to be important for retigabine and ML-213 binding, and their immediate neighbors, followed by energy minimization using the GROMOS 43B1 force field (3), in DeepView (4). Thus, we converted the *Xenopus laevis* KCNQ1 amino acid sequence LITTLYIGF to LITAWYIGF, the underlined W being W270 in human KCNQ5 and the italicized residues being the immediate neighbors in KCNQ5. In addition, we converted the *Xenopus laevis* KCNQ1 sequence WWGVVTVTIGYGD to WWGLITLATIGYGD to better reflect human KCNQ3/KCNQ5. Surrounding non-mutated sequences are shown to illustrate the otherwise high sequence identity in these stretches. We then performed unguided docking of aloperine using SwissDock (5) with CHARMM forcefields (6).

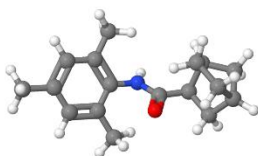
Supplementary references

1. Mulvany MJ & Halpern W (1977) Contractile properties of small arterial resistance vessels in spontaneously hypertensive and normotensive rats. *Circulation research* 41(1):19-26.
2. Sun J & MacKinnon R (2017) Cryo-EM Structure of a KCNQ1/CaM Complex Reveals Insights into Congenital Long QT Syndrome. *Cell* 169(6):1042-1050 e1049.
3. van Gunsteren WF (1996) *Biomolecular simulation: the GROMOS96 manual and user guide*. (Vdf Hochschulverlag ETHZ).
4. Johansson MU, Zoete V, Michielin O, & Guex N (2012) Defining and searching for structural motifs using DeepView/Swiss-PdbViewer. *BMC bioinformatics* 13:173.
5. Grosdidier A, Zoete V, & Michielin O (2011) SwissDock, a protein-small molecule docking web service based on EADock DSS. *Nucleic acids research* 39(Web Server issue):W270-277.
6. Grosdidier A, Zoete V, & Michielin O (2011) Fast docking using the CHARMM force field with EADock DSS. *Journal of computational chemistry* 32(10):2149-2159.

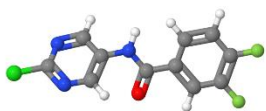
Supplementary Figures



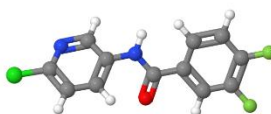
retigabine



ML213



ICA-069673

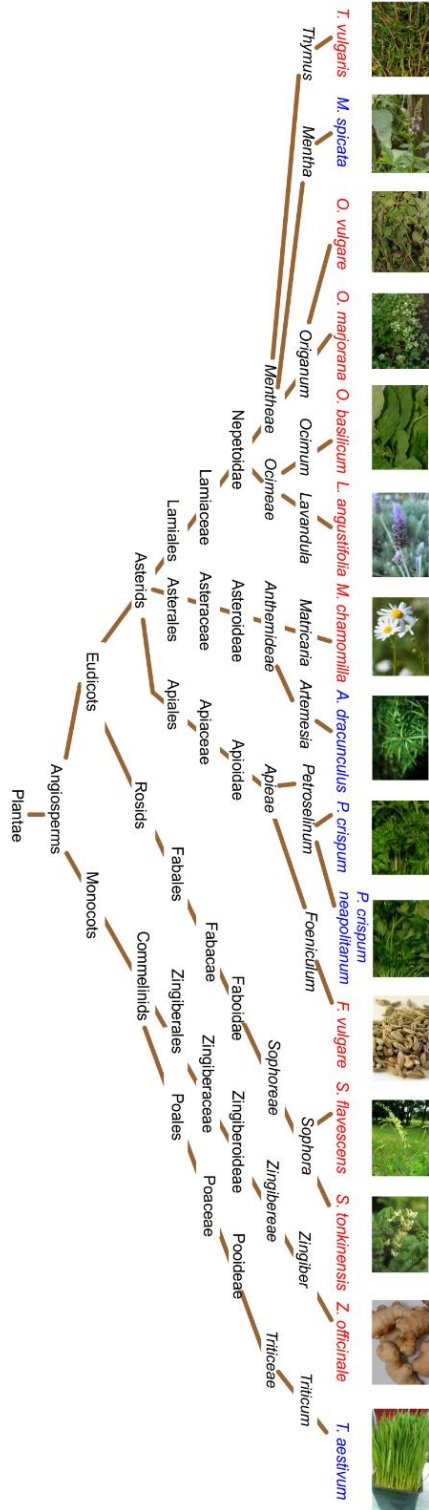


ICA-27243

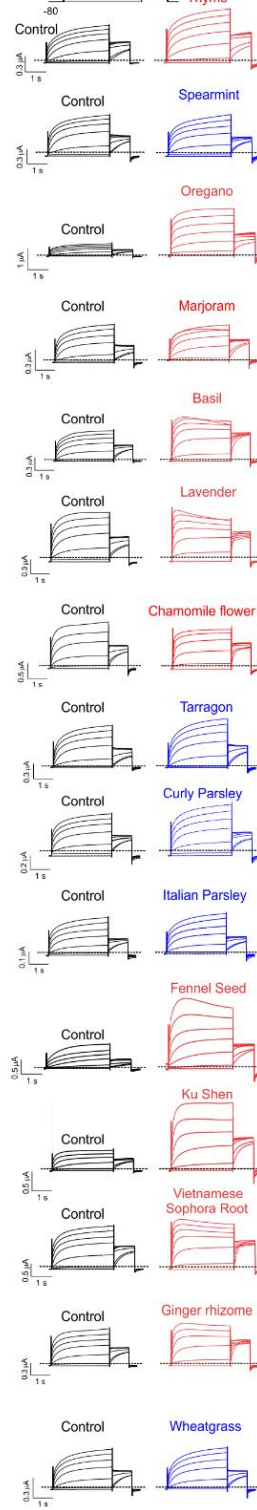
Fig. S1. Structures of retigabine and related compounds.

Blue, nitrogen; gray, carbon; green, fluorine; red, oxygen; white, hydrogen.

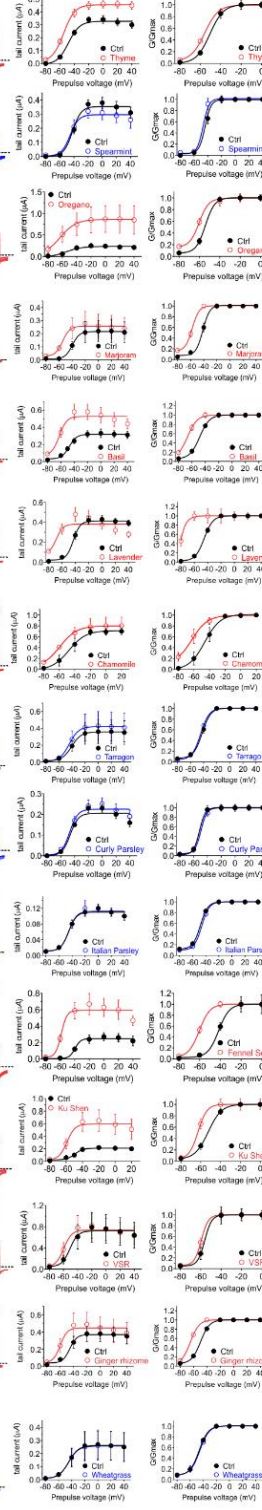
A



B



C



D

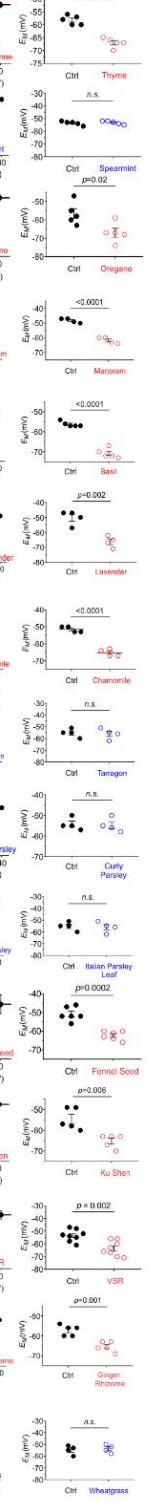


Fig. S2. KCNQ5 activation is a specific, shared feature of botanical hypotensive folk medicines.

All error bars indicate SEM.

A. Left, Phylogenetic tree showing relationships of the plants examined in this study. Red, plants previously reported to show hypotensive activity or used traditionally as hypotensives; blue, non-hypotensives or diuretic hypotensives (here and panels B-D). Right, images of the plants used (for attributions see Supplementary Materials).

B. Mean TEVC current traces for KCNQ5 expressed in *Xenopus* oocytes in the absence (control) or presence of 1% extract from the medicinal plants as indicated ($n = 4-8$). Dashed line here and throughout, zero current level. *Upper inset*, the voltage protocol used here and throughout the study unless otherwise indicated. Arrow indicates time point at which tail currents are measured throughout this study.

C. Mean tail current (left) and normalized tail currents (G/G_{max}) (right) versus prepulse voltage relationships for the traces as in B ($n = 4-8$).

D. Effects of the hypotensive plant extracts on resting membrane potential (E_M) of unclamped oocytes expressing KCNQ5 ($n = 4-8$).

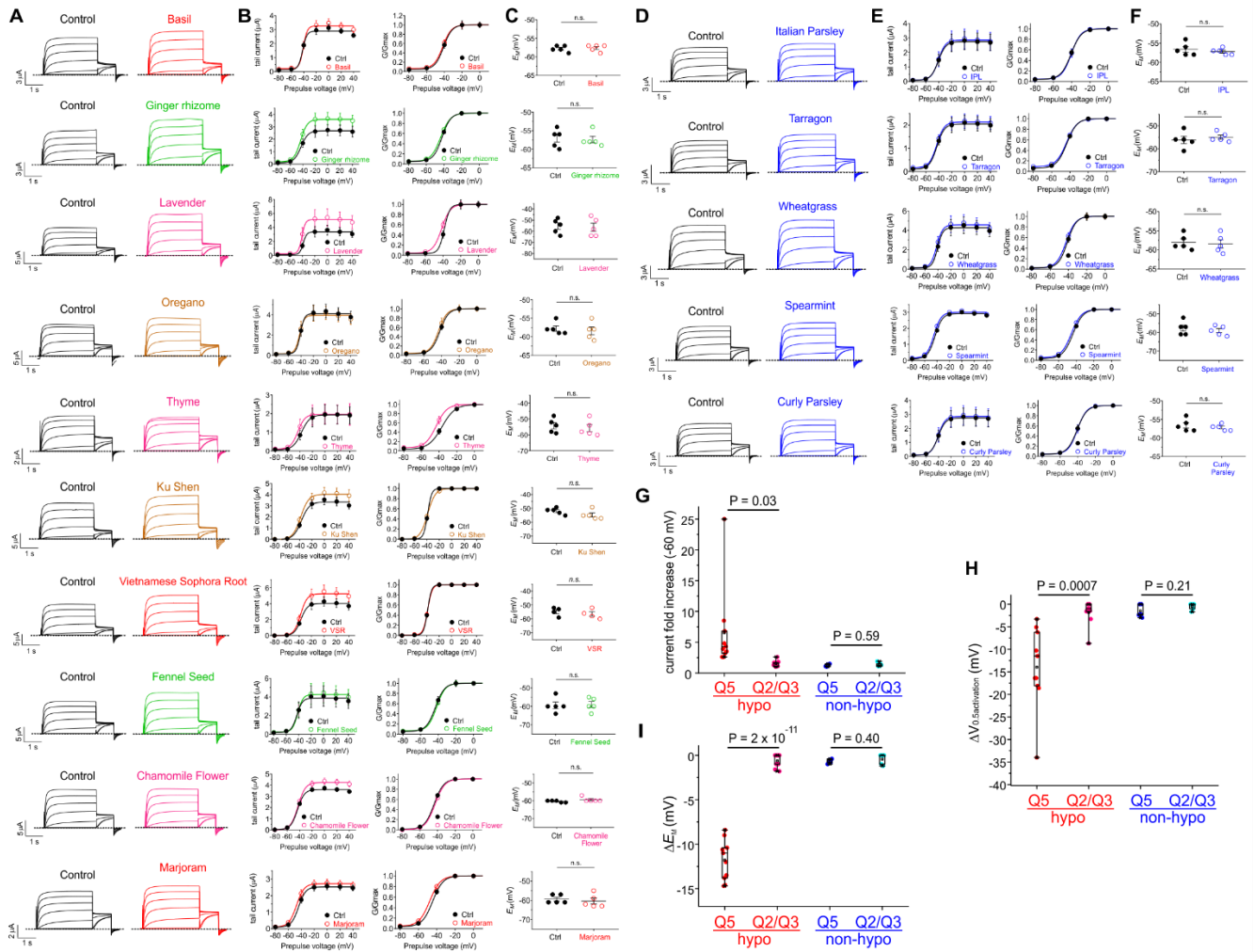


Fig. S3. KCNQ2/3 is relatively insensitive to botanical hypotensive folk medicines

All error bars indicate SEM.

A. Mean TEVC current traces for KCNQ2/3 channels expressed in *Xenopus* oocytes in the absence (control) or presence of 1% extract from the hypotensive plants as indicated ($n = 5$).

B. Mean tail current (*left*) and normalized tail currents (G/G_{max}) (*right*) versus prepulse voltage relationships for the traces as in A ($n = 5$).

C. Effects of the hypotensive plant extracts indicated on resting membrane potential (E_M) of unclamped oocytes expressing KCNQ2/3 channels ($n = 5$).

D. Mean TEVC current traces for KCNQ2/3 channels expressed in *Xenopus* oocytes in the absence (control) or presence of 1% extract from the non-hypotensive plants as indicated ($n = 5$).

E. Mean tail current (*left*) and normalized tail currents (G/G_{max}) (*right*) versus prepulse voltage relationships for the traces as in D ($n = 5$).

F. Effects of the non-hypotensive plant extracts indicated on resting membrane potential (E_M) of unclamped oocytes expressing KCNQ2/3 channels ($n = 5$).

G-I. Mean effects of hypotensive (red/pink) versus non-hypotensive plant extracts (blue/cyan) (1%) on (G) current at -60 mV, (H) $V_{0.5activation}$, (I) E_M on KCNQ5 versus KCNQ2/3 ($n = 5$). Each point represents the mean data from one plant species. KCNQ5 data are repeated from Figure 1 and Fig. S2.

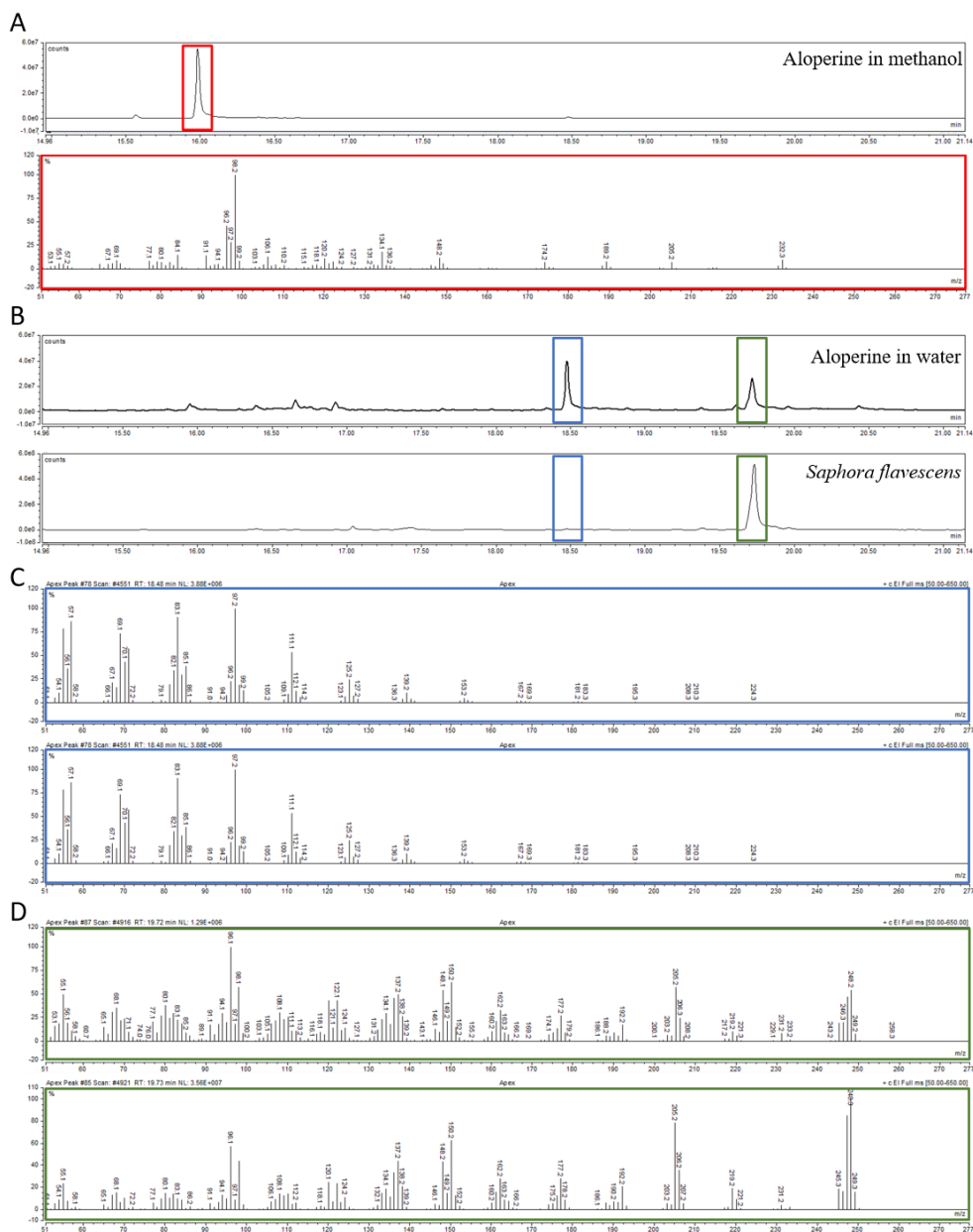


Fig. S4. GC/MS analysis of aloperine in *S. flavescens* extract

A. Chromatogram of aloperine dissolved in methanol, diluted in dichloromethane (DCM) to a concentration of 25 μ M (top) aloperine with <1% methanol. The mass spectrum of the main peak (boxed in red) with a retention time of 16.0 minutes is shown underneath.

B Comparison of the chromatograms of aloperine extracted using DCM from an aqueous solution (top) and the chromatogram produced by the DCM extraction of the *S. flavescens* extract (bottom).

C. Comparison of spectra seen in the first peak (boxed in blue) with the retention time of 18.5 minutes, (top: aloperine standard; bottom: *S. flavescens* extract).

D. Comparison of spectra of the later peak (19.7-minute retention time, boxed in green),

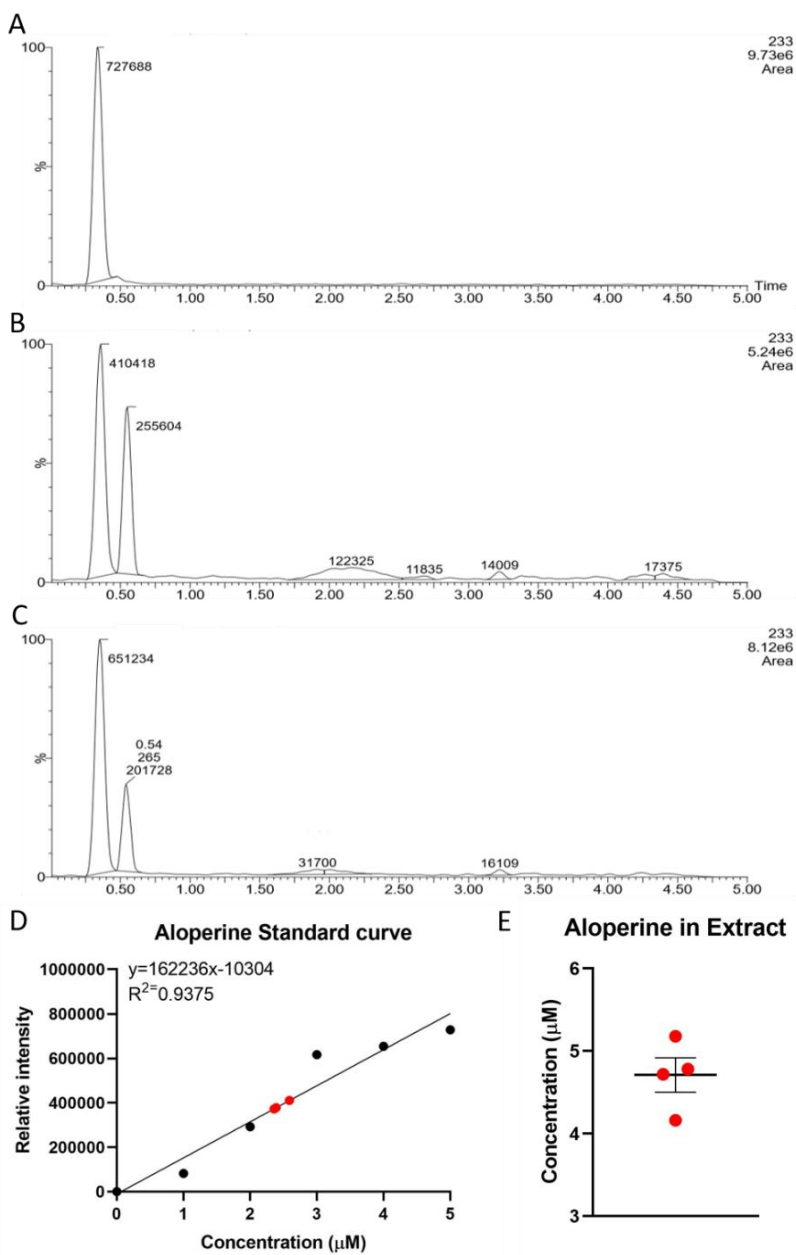


Fig. S5. LC/MS analysis of aloperine in *S. flavescens* extract

A-C. Extracted ion chromatograms for the 233 Da mass with the calculated intensities labelling the peaks: A. 5 μM aloperine standard; B. *S. flavescens* extract; C. *S. flavescens* extract with 2 μM aloperine added to the sample.

D. The standard curve produced by integrated peaks from the standards (1 μM - 5 μM , in 1 μM increments). The red dots refer to the 1:2 dilutions of *S. flavescens* extract, with the molarities calculated based off the equation for the standard curve.

E. The corrected values for the minimum concentration of aloperine in the undiluted extract (4.71 μM +/- 0.21 μM).

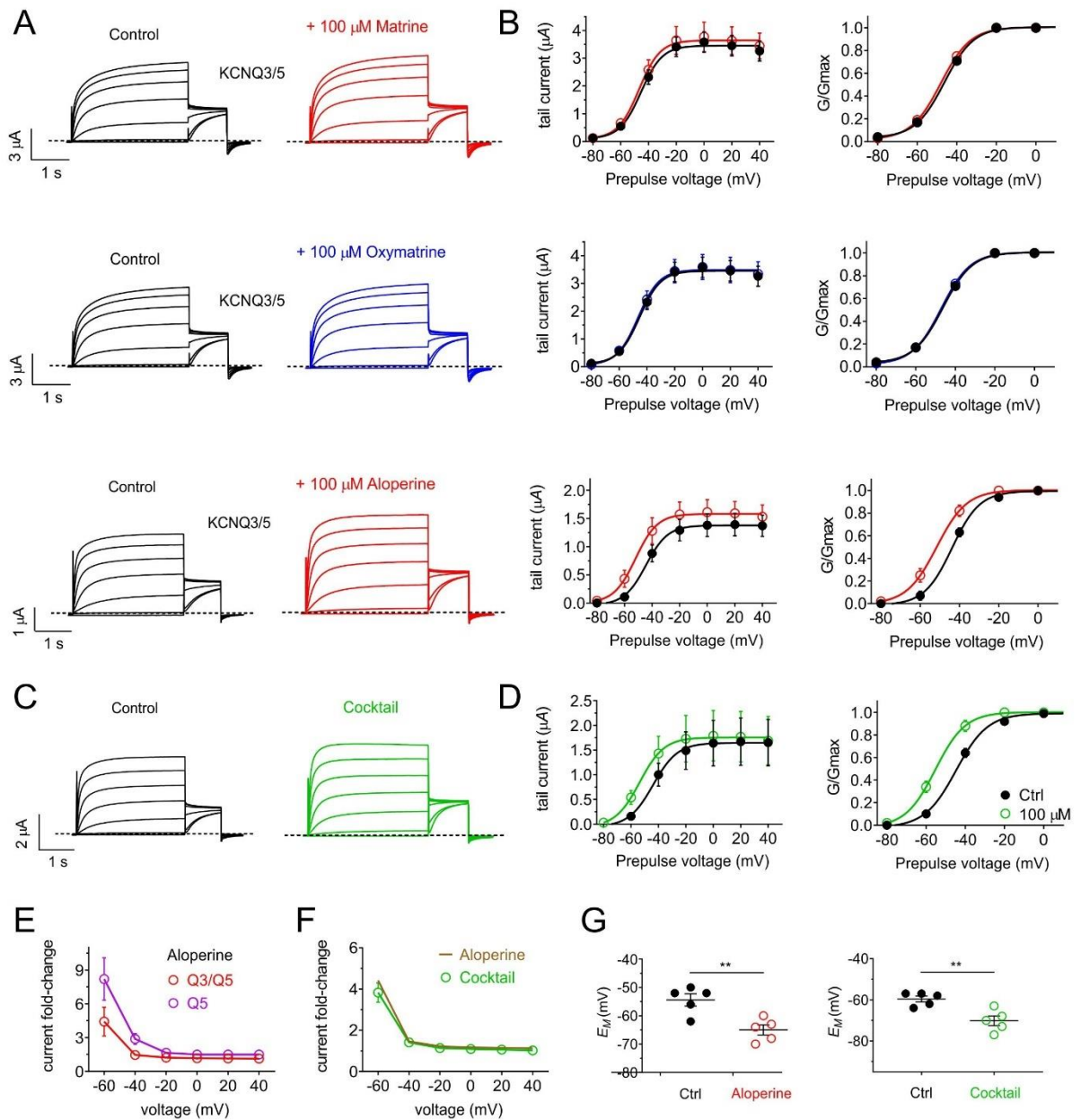


Fig. S6. Effects of aloperine, matrine and oxymatrine on heteromeric KCNQ3/5 activity.

All error bars indicate SEM.

A. Mean TEVC current traces showing effects of compounds as indicated (100 μ M) on KCNQ3/5 expressed in *Xenopus* oocytes ($n = 5$).

B. Mean tail current (left) and mean normalized tail currents (G/Gmax) (right) versus prepulse voltage relationships for the traces as in A ($n = 5$).

- C. Mean TEVC current traces showing effects of aloperine, matrine and oxymatrine (1 μM each) in combination (cocktail) on KCNQ3/5 expressed in *Xenopus* oocytes ($n = 5$).
- D. Mean tail current (left) and mean normalized tail currents (G/Gmax) (right) versus prepulse voltage relationships for the traces as in C ($n = 5$).
- E. Comparison of effects of aloperine (100 μM) on KCNQ5 versus KCNQ3/5 calculated from fold increase in current at -60 mV; $n = 5$.
- F. Comparison of effects of aloperine (100 μM) versus the cocktail on KCNQ3/5 calculated from fold increase in current at -60 mV; $n = 5$.
- G. Effects of aloperine (100 μM) versus the cocktail on resting membrane potential (E_M) of unclamped oocytes expressing KCNQ3/5 ($n = 5$); **P < 0.01.

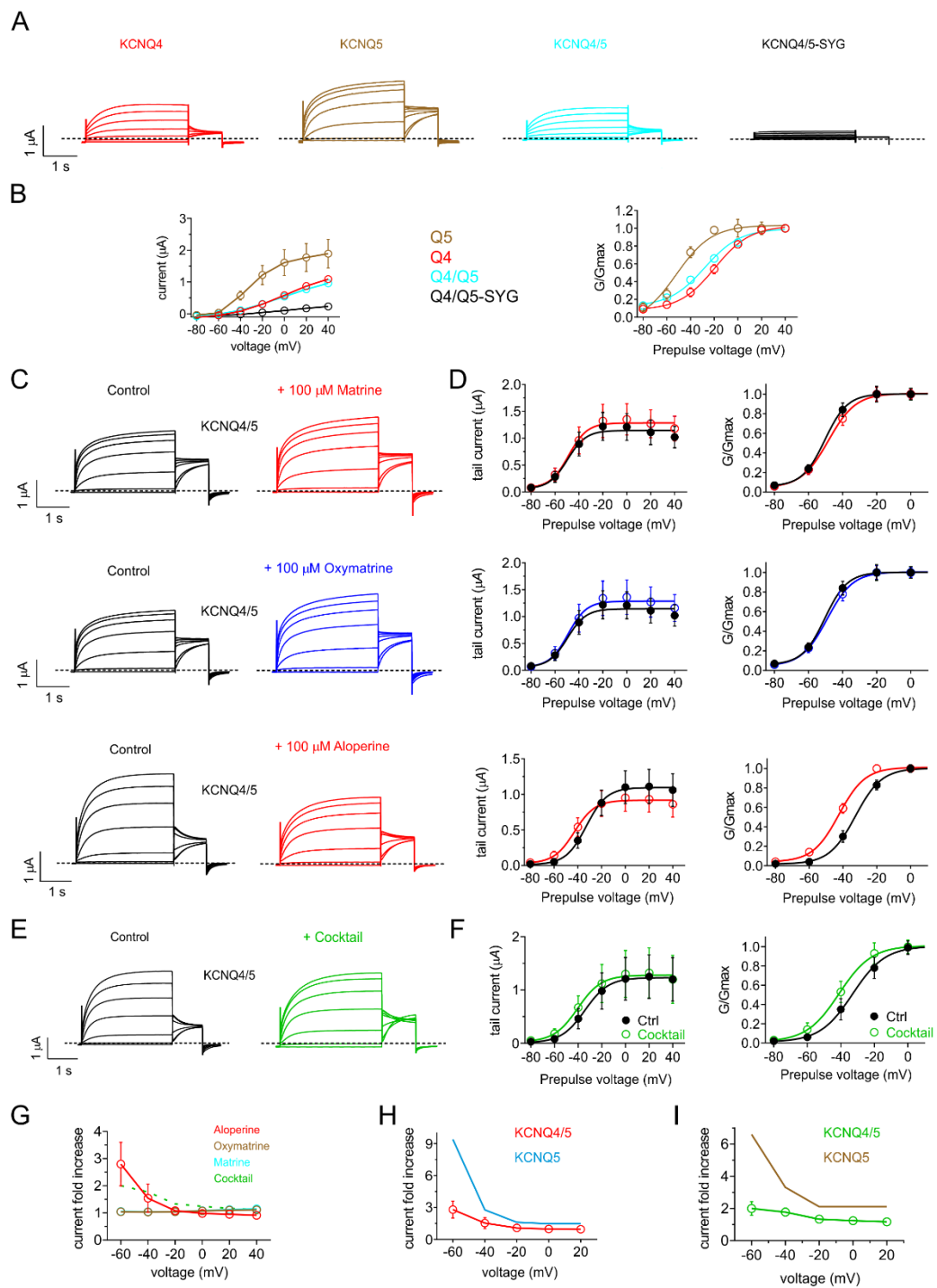


Fig. S7. Effects of aloperine, matrine and oxymatrine on heteromeric KCNQ4/5 activity. All error bars indicate SEM.

A. Mean TEVC current traces for wild-type KCNQ4, KCNQ5 and KCNQ5-SYG alone and/or together as indicated, expressed in *Xenopus* oocytes ($n = 5-10$).

- B. Mean tail current (left) and mean normalized tail currents (G/Gmax) (right) versus prepulse voltage relationships for the traces as in A ($n = 5-10$).
- C. Mean TEVC current traces showing effects of compounds as indicated (100 μ M) on KCNQ4/5 expressed in *Xenopus* oocytes ($n = 6-8$).
- D. Mean tail current (left) and mean normalized tail currents (G/Gmax) (right) versus prepulse voltage relationships for the traces as in A ($n = 6-8$).
- E. Mean TEVC current traces showing effects of aloperine, matriline and oxymatriline (1 μ M each) in combination (cocktail) on KCNQ4/5 expressed in *Xenopus* oocytes ($n = 4$).
- F. Mean tail current (left) and mean normalized tail currents (G/Gmax) (right) versus prepulse voltage relationships for the traces as in C ($n = 4$).
- G. Comparison of effects of compounds shown (100 μ M) versus the cocktail on KCNQ4/5 calculated from fold increase in current at -60 mV; $n = 4-8$.
- H. Comparison of effects of aloperine (100 μ M) on KCNQ5 versus KCNQ4/5 calculated from fold increase in current at -60 mV; $n = 5-8$.
- I. Comparison of effects of the cocktail on KCNQ5 versus KCNQ4/5 calculated from fold increase in current at -60 mV; $n = 4-5$.

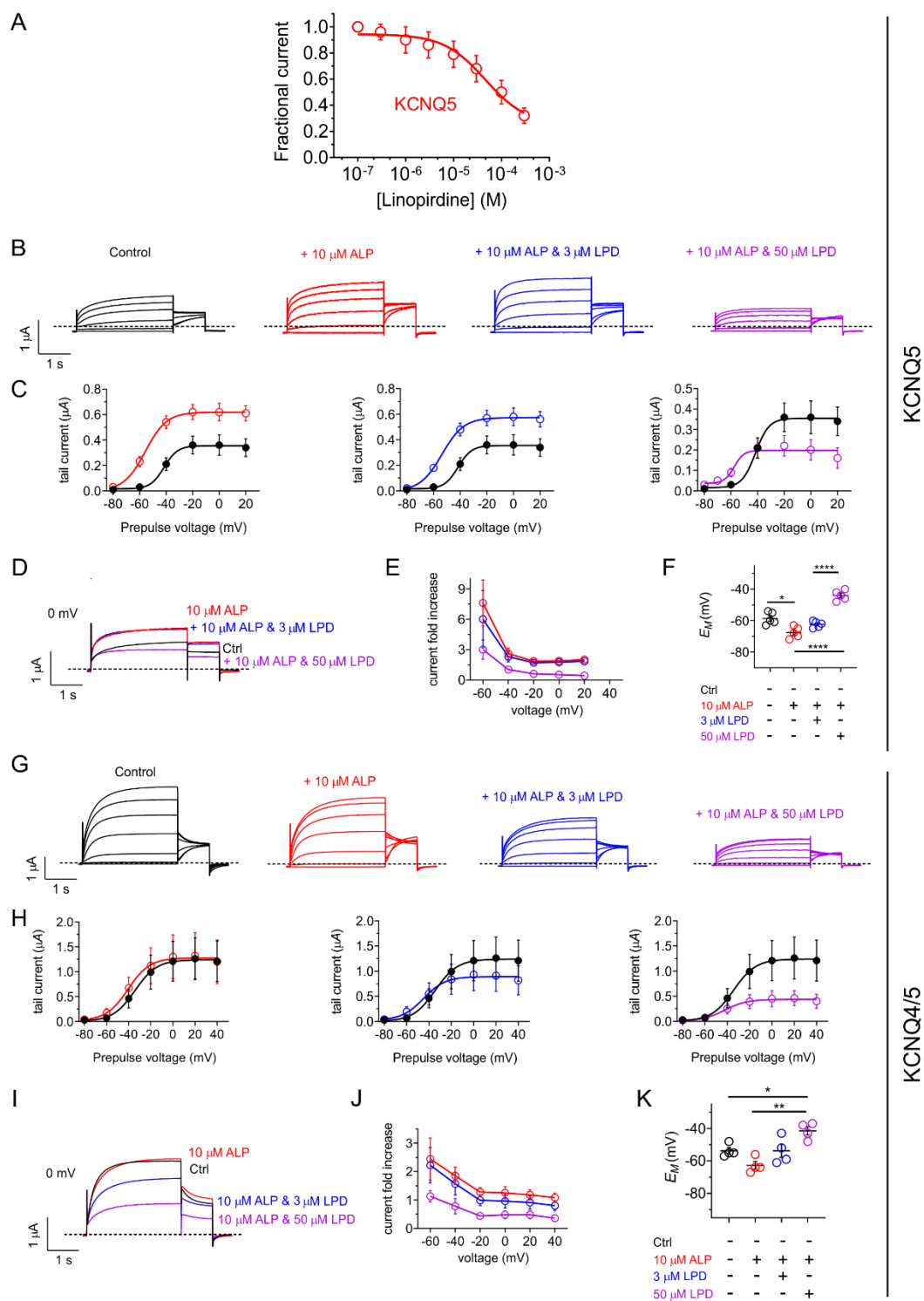


Fig. S8. Effects of linopirdine on alopirdine modulation of KCNQ5 and KCNQ4/5.

A. Fractional KCNQ5 current in response to different doses of linopirdine ($n = 6$).

- B. Mean TEVC current traces showing effects of linopirdine on aloperine activation of KCNQ5 expressed in *Xenopus* oocytes ($n = 5$).
- C. Mean tail current versus prepulse voltage relationships for the traces as in D ($n = 5$).
- D. Mean TEVC current traces at 0 mV prepulse overlaid to show effects of linopirdine on aloperine activation of KCNQ5 expressed in *Xenopus* oocytes ($n = 5$).
- E. Mean effects of linopirdine on aloperine activation of KCNQ5 expressed in *Xenopus* oocytes shown as current fold-change at -60 mV ($n = 5$).
- F. Mean effects of linopirdine on aloperine KCNQ5-dependently shifting the resting membrane potential (E_M) of unclamped oocytes ($n = 5$). * $P < 0.05$; **** $P < 0.0001$.
- G. Mean TEVC current traces showing effects of linopirdine on aloperine activation of KCNQ4/5 expressed in *Xenopus* oocytes ($n = 5$).
- H. Mean tail current versus prepulse voltage relationships for the traces as in I ($n = 5$).
- I. Mean TEVC current traces at 0 mV prepulse overlaid to show effects of linopirdine on aloperine activation of KCNQ4/5 expressed in *Xenopus* oocytes ($n = 5$).
- J. Mean effects of linopirdine on aloperine activation of KCNQ4/5 expressed in *Xenopus* oocytes shown as current fold-change at -60 mV ($n = 5$).
- K. Mean effects of linopirdine on aloperine KCNQ4/5-dependently shifting the resting membrane potential (E_M) of unclamped oocytes ($n = 5$). * $P < 0.05$; ** $P < 0.01$.

Supplementary Tables

KCNQ5 activation $V_{0.5}$ (mV)		KCNQ5 activation slope (mV)	
Control -48.5 ± 1.5 (n=5)	1:100 Basil -66.6 ± 2.3 (n=5) ***	Control 7.4 ± 0.7 (n=5)	1:100 Basil 6.3 ± 1.5 (n=5)
Control -48.4 ± 1.3 (n=5)	1:100 Ginger -59.9 ± 0.9 (n=5) ***	Control 6.9 ± 0.7 (n=5)	1:100 Ginger 6.4 ± 1.3 (n=5)
Control -44.9 ± 3.4 (n=5)	1:100 Lavender -78.9 ± 3.0 (n=5) ****	Control 7.2 ± 1.0 (n=5)	1:100 Lavender 6.2 ± 1.6 (n=5)
Control -54.1 ± 1.9 (n=5)	1:100 Oregano -60.3 ± 1.2 (n=5) *	Control 4.6 ± 1.3 (n=5)	1:100 Oregano 8.2 ± 3.4 (n=5)
Control -51.5 ± 2.4 (n=5)	1:100 Curly Parsley -49.3 ± 2.5 (n=5)	Control 3.8 ± 1.3 (n=5)	1:100 Curly Parsley 4.3 ± 0.9 (n=5)
Control -43.9 ± 0.9 (n=5)	1:100 Spearmint -46.9 ± 1.2 (n=5)	Control 6.3 ± 1.1 (n=5)	1:100 Spearmint 2.9 ± 0.8 (n=5)
Control -50.6 ± 1.5 (n=5)	1:100 Thyme -55.7 ± 1.4 (n=5) *	Control 6.0 ± 2.0 (n=5)	1:100 Thyme 7.9 ± 0.7 (n=5)
Control -56.1 ± 1.1 (n=8)	1:100 <i>S. tonkinensis</i> -59.4 ± 1.4 (n=8)	Control 3.5 ± 6.2 (n=8)	1:100 <i>S. tonkinensis</i> 3.4 ± 5.2 (n=8)
Control -52.4 ± 1.3 (n=5)	1:100 <i>S. flavescens</i> -62.7 ± 1.8 (n=5) **	Control 6.7 ± 0.8 (n=5)	1:100 <i>S. flavescens</i> 4.5 ± 1.7 (n=5)
Control -41.7 ± 2.4 (n=5)	1:100 Fennel Seed -60.3 ± 2.6 (n=5) ***	Control 5.9 ± 2.8 (n=5)	1:100 Fennel Seed 5.2 ± 2.3 (n=5)
Control -46.1 ± 3.6 (n=5)	1:100 Chamomile -62.5 ± 5.6 (n=5) *	Control 9.5 ± 3.2 (n=5)	1:100 Chamomile 12.3 ± 7.6 (n=5)
Control -48.2 ± 0.9 (n=4)	1:100 Italian parsley leaf -46.1 ± 0.8 (n=4)	Control 5.8 ± 0.5 (n=4)	1:100 Italian parsley leaf 5.7 ± 0.7 (n=4)
Control -41.1 ± 1.0 (n=4)	1:100 Marjoram -57.5 ± 1.3 (n=4) ***	Control 6.8 ± 1.8 (n=4)	1:100 Marjoram 7.0 ± 0.7 (n=4)
Control -42.2 ± 0.9 (n=4)	1:100 Tarragon -44.6 ± 1.1 (n=4)	Control 6.6 ± 1.7 (n=4)	1:100 Tarragon 6.6 ± 0.6 (n=4)
Control -46.4 ± 1.2 (n=4)	1:100 Wheatgrass -45.2 ± 1.2 (n=4)	Control 6.6 ± 0.8 (n=4)	1:100 Wheatgrass 7.5 ± 1.2 (n=4)

Table S1. Summary of the effects of herbal extracts on KCNQ5 channels.

Each line shows mean values for voltage dependence of channel activation in the presence of herb extract and the corresponding mean values for the same oocytes in the absence of extract (Control). Values were obtained from a Boltzmann fit of the normalized tail current versus prepulse voltage. Statistics versus same channel in absence of herbal extract: * $p < 0.05$; ** $p < 0.01$; *** $p < 0.001$; **** $p < 0.0001$. Values indicate mean ± SEM.

KCNQ2/3 activation $V_{0.5}$ (mV)		KCNQ2/3 activation slope (mV)	
Control -40.9 ± 1.3 (n=5)	1:100 Basil -41.9 ± 1.4 (n=5)	Control 4.8 ± 3.4 (n=5)	1:100 Basil 4.9 ± 2.5 (n=5)
Control -42.2 ± 0.5 (n=5)	1:100 Ginger -43.7 ± 0.8 (n=5)	Control 4.9 ± 0.9 (n=5)	1:100 Ginger 5.2 ± 0.9 (n=5)
Control -42.2 ± 4.7 (n=5)	1:100 Lavender -43.7 ± 1.3 (n=5)	Control 3.1 ± 1.1 (n=5)	1:100 Lavender 4.9 ± 2.5 (n=5)
Control -41.9 ± 1.1 (n=5)	1:100 Oregano -43.5 ± 2.6 (n=5)	Control 4.9 ± 1.1 (n=5)	1:100 Oregano 4.7 ± 2.6 (n=5)
Control -41.8 ± 0.5 (n=5)	1:100 Curly Parsley -42.6 ± 0.6 (n=5)	Control 4.9 ± 0.9 (n=5)	1:100 Curly Parsley 5.2 ± 0.9 (n=5)
Control -43.8 ± 0.5 (n=5)	1:100 Spearmint -45.5 ± 0.8 (n=5)	Control 5.7 ± 0.6 (n=5)	1:100 Spearmint 5.7 ± 0.7 (n=5)
Control -36.8 ± 1.1 (n=5)	1:100 Thyme -43.4 ± 1.4 (n=5)	Control 7.5 ± 1.1 (n=5)	1:100 Thyme 6.1 ± 1.6 (n=5)
Control -37.4 ± 0.5 (n=5)	1:100 <i>S. tonkinensis</i> -37.2 ± 0.6 (n=5)	Control 4.5 ± 0.8 (n=5)	1:100 <i>S. tonkinensis</i> 5.8 ± 0.8 (n=5)
Control -37.9 ± 0.8 (n=5)	1:100 <i>S. flavescens</i> -37.8 ± 0.9 (n=5)	Control 4.0 ± 1.5 (n=5)	1:100 <i>S. flavescens</i> 7.2 ± 1.0 (n=5)
Control -43.4 ± 1.6 (n=5)	1:100 Fennel Seed -41.9 ± 1.1 (n=5)	Control 5.2 ± 1.9 (n=5)	1:100 Fennel Seed 4.9 ± 1.9 (n=5)
Control -43.9 ± 0.6 (n=5)	1:100 Chamomile -42.9 ± 0.4 (n=5)	Control 5.4 ± 0.6 (n=5)	1:100 Chamomile 5.5 ± 0.6 (n=5)
Control -40.7 ± 0.6 (n=5)	1:100 Italian parsley leaf -40.4 ± 0.8 (n=5)	Control 5.3 ± 1.3 (n=5)	1:100 Italian parsley leaf 5.1 ± 2.0 (n=5)
Control -44.4 ± 0.8 (n=5)	1:100 Marjoram -47.7 ± 0.8 (n=5)	Control 5.7 ± 0.8 (n=5)	1:100 Marjoram 5.8 ± 0.8 (n=5)
Control -43.4 ± 0.6 (n=5)	1:100 Tarragon -43.8 ± 0.9 (n=5)	Control 5.8 ± 0.7 (n=5)	1:100 Tarragon 5.7 ± 1.0 (n=5)
Control -41.1 ± 1.2 (n=5)	1:100 Wheatgrass -42.6 ± 1.3 (n=5)	Control 4.8 ± 2.8 (n=5)	1:100 Wheatgrass 5.2 ± 1.9 (n=5)

Table S2. Summary of the effects of herbal extracts on KCNQ2/3 channels.

Each line shows mean values for voltage dependence of channel activation in the presence of herb extract and the corresponding mean values for the same oocytes in the absence of extract (Control). Values were obtained from a Boltzmann fit of the normalized tail current versus prepulse voltage. None of the effects achieved a p value < 0.05. Values indicate mean ± SEM.

KCNQ5	Normalized tail current $V_{0.5}$ (mV)	Slope (mV)
Control	-31.2 ± 0.3 (n =5)	7.7 ± 0.2 (n =5)
0.1 μ M	-38.9 ± 0.9 (n =5) ***	10.5 ± 0.8 (n =5)
1 μ M	-41.7 ± 0.9 (n =5) ****	8.9 ± 1.0 (n =5)
10 μ M	-42.8 ± 0.7 (n =5) ****	7.1 ± 0.8 (n =5)
100 μ M	-44.7 ± 0.7 (n =5) ****	6.7 ± 0.6 (n =5)
1 mM	-48.9 ± 0.6 (n =5) ****	5.6 ± 0.3 (n =5)

Table S3. Summary of effects of aloperine on KCNQ5 channels.

Statistics versus same channel in absence of aloperine: ****p<0.0001, ***p=0.0009. Values indicate mean \pm SEM.

KCNQ2/3	Normalized tail current $V_{0.5}$ (mV)	Slope (mV)
Control	-41.8 ± 0.6 (n =5)	5.7 ± 0.9 (n =5)
0.1 μ M	-43.2 ± 0.7 (n =5)	5.8 ± 0.8 (n =5)
1 μ M	-44.1 ± 0.7 (n =5)	5.9 ± 0.7 (n =5)
10 μ M	-44.6 ± 0.7 (n =5)	5.9 ± 0.7 (n =5)
100 μ M	-44.4 ± 0.8 (n =5)	5.9 ± 0.8 (n =5)
1 mM	-43.3 ± 0.8 (n =5)	5.8 ± 0.9 (n =5)

Table S4. Summary of effects of aloperine on KCNQ2/3 channels.

Statistics versus same channel in absence of aloperine. Values indicate mean \pm SEM.

KCNQ3/5	Non-normalized tail current $V_{0.5}$ (mV)	Slope (mV)
Control	-44.4 ± 2.8 (n =5)	7.8 ± 2.8 (n =5)
100 μM alopérine	-51.9 ± 4.8 (n =5)	7.9 ± 2.0 (n =5)

Table S5. Summary of effects of alopérine on KCNQ3/5 channels.

Statistics versus same channel in absence of alopérine. Values indicate mean ± SEM.

KCNQ3/5	Non-normalized tail current $V_{0.5}$ (mV)	Slope (mV)
Control	-43.8 ± 4.4 (n =5)	8.8 ± 2.6 (n =5)
Cocktail	-53.7 ± 4.9 (n =5)	9.0 ± 6.5 (n =5)

Table S6. Summary of effects of cocktail on KCNQ3/5 channels.

Statistics versus same channel in absence of cocktail. Values indicate mean ± SEM.

KCNQ4/5	Non-normalized tail current $V_{0.5}$ (mV)	Slope (mV)
Control	-32.8 ± 6.1 (n =8)	8.6 ± 4.1 (n =8)
100 μM alopérine	-42.8 ± 7.4 (n =8)	8.3 ± 4.2 (n =8)

Table S7. Summary of effects of alopérine on KCNQ4/5 channels.

Statistics versus same channel in absence of alopérine. Values indicate mean ± SEM.

KCNQ4/5	Non-normalized tail current $V_{0.5}$ (mV)	Slope (mV)
Control	-34.2 ± 1.5 (n =4)	9.9 ± 2.5 (n =4)
Cocktail	-40.5 ± 1.5 (n =4) *	10.0 ± 2.3 (n =4)

Table S8. Summary of effects of cocktail on KCNQ4/5 channels.

Statistics versus same channel in absence of cocktail. *p=0.025. Values indicate mean ± SEM.

KCNQ2	Normalized tail current $V_{0.5}$ (mV)	Non-normalized tail current $V_{0.5}$ (mV)	Slope (mV)
Control	-42.4 ± 1.9 (n =5)	-43.8 ± 6.5 (n =5)	7.1 ± 2.1 (n =5)
0.1 μM	-46.1 ± 0.9 (n =5)	-46.7 ± 7.4 (n =5)	5.1 ± 0.6 (n =5)
1 μM	-47.3 ± 0.7 (n =5)	-47.2 ± 7.1 (n =5)	5.2 ± 0.4 (n =5)
10 μM	-47.7 ± 0.6 (n =5)	-47.3 ± 7.0 (n =5)	5.1 ± 0.6 (n =5)
100 μM	-48.1 ± 1.6 (n =5)	-47.5 ± 7.0 (n =5)	5.5 ± 0.8 (n =5)
1 mM	-48.8 ± 2.0 (n =5)	-47.0 ± 8.0 (n =5)	4.5 ± 0.9 (n =5)

Table S9. Summary of effects of aloperine on KCNQ2 channels.

Statistics versus same channel in absence of aloperine. Values indicate mean ± SEM.

KCNQ3*	Normalized tail current $V_{0.5}$ (mV)	Non-normalized tail current $V_{0.5}$ (mV)	Slope (mV)
Control	-45.7 ± 1.2 (n =5)	-45.3 ± 6.1 (n =5)	n.a.
0.1 μM	-47.3 ± 1.3 (n =5)	-46.7 ± 6.3 (n =5)	n.a.
1 μM	-48.5 ± 1.3 (n =5)	-47.9 ± 6.3 (n =5)	n.a.
10 μM	-48.2 ± 1.4 (n =5)	-47.6 ± 6.4 (n =5)	n.a.
100 μM	-47.8 ± 1.8 (n =5)	-47.7 ± 6.6 (n =5)	n.a.
1 mM	-48.6 ± 1.3 (n =5)	-47.1 ± 6.6 (n =5)	n.a.

Table S10. Summary of effects of aloperine on KCNQ3* channels.

Statistics versus same channel in absence of aloperine. Values indicate mean ± SEM.

KCNQ4	Normalized tail current $V_{0.5}$ (mV)	Non-normalized tail current $V_{0.5}$ (mV)	Slope (mV)
Control	-2.2 ± 0.8 (n =5)	-2.7 ± 5.6 (n =5)	13.5 ± 0.5 (n =5)
0.1 μM	-7.0 ± 0.8 (n =5) **	-7.9 ± 5.4 (n =5)	13.5 ± 0.5 (n =5)
1 μM	-13.2 ± 1.4 (n =5) ***	-13.7 ± 4.3 (n =5)	13.3 ± 1.3 (n =5)
10 μM	-13.7 ± 1.3 (n =5) ***	-14.4 ± 5.2 (n =5)	14.2 ± 1.3 (n =5)
100 μM	-14.8 ± 1.2 (n =5) ****	-15.5 ± 4.7 (n =5)	14.4 ± 1.2 (n =5)
1 mM	-16.0 ± 0.9 (n =5) ****	-16.2 ± 4.7 (n =5)	13.3 ± 0.9 (n =5)

Table S11. Summary of effects of aloperine on KCNQ4 channels.

Statistics versus same channel in absence of aloperine: **p=0.004, *p=0.05. Values indicate mean ± SEM.

KCNQ1	Normalized tail current $V_{0.5}$ (mV)	Non-normalized tail current $V_{0.5}$ (mV)	Slope (mV)
Control	-21.6 ± 0.5 (n =5)	-21.6 ± 2.0 (n =5)	8.9 ± 0.5 (n =5)
0.1 μM	-27.3 ± 1.5 (n =5) *	-26.1 ± 4.5 (n =5)	7.9 ± 1.2 (n =5)
1 μM	-27.6 ± 1.5 (n =5) *	-28.2 ± 3.7 (n =5)	8.9 ± 1.2 (n =5)
10 μM	-29.6 ± 1.3 (n =5) **	-30.6 ± 3.8 (n =5)	8.8 ± 1.3 (n =5)
100 μM	-31.3 ± 0.9 (n =5) ****	-31.4 ± 3.2 (n =5)	8.1 ± 0.7 (n =5)
1 mM	-32.6 ± 0.9 (n =5) ****	-31.6 ± 1.9 (n =5)	6.9 ± 0.6 (n =5)

Table S12. Summary of effects of aloperine on KCNQ1 channels.

Statistics versus same channel in absence of aloperine: ****p<0.0001, **p=0.004, *p=0.05. Values indicate mean ± SEM.

KCNQ1/KCNE1	Normalized tail current $V_{0.5}$ (mV)	Non-normalized tail current $V_{0.5}$ (mV)	Slope (mV)
Control	63.1 ± 1.2 (n =5)	63.3 ± 5.2 (n =5)	23.6 ± 0.7 (n =5)
0.1 μM	60.2 ± 1.0 (n =5)	58.8 ± 8.1 (n =5)	23.4 ± 0.7 (n =5)
1 μM	58.5 ± 1.2 (n =5)	57.2 ± 8.8 (n =5)	24.1 ± 0.8 (n =5)
10 μM	55.9 ± 1.2 (n =5)	55.2 ± 8.9 (n =5)	24.4 ± 0.9 (n =5)
100 μM	53.6 ± 0.8 (n =5)	53.4 ± 5.7 (n =5)	24.6 ± 0.5 (n =5)
1 mM	48.5 ± 0.8 (n =5)	48.7 ± 5.9 (n =5)	21.8 ± 0.6 (n =5)

Table S13. Summary of effects of aloperine on KCNQ1/KCNE1 channels.

Statistics versus same channel in absence of aloperine. Values indicate mean ± SEM.

KCNQ1/KCNE3	Normalized tail current $V_{0.5}$ (mV)	Non-normalized tail current $V_{0.5}$ (mV)	Slope (mV)
Control	-57.1 ± 19.4 (n =5)	-51.6 ± 88 (n =5)	16.9 ± 16.5 (n =5)
Aloperine	-91.7 ± 159 (n =5)	-49.0 ± 96 (n =5)	16.2 ± 57.2 (n =5)

Table S14. Summary of effects of aloperine on KCNQ1/KCNE3 channels.

Statistics versus same channel in absence of aloperine. Values indicate mean ± SEM.

KCNQ5-R212A	Normalized tail current $V_{0.5}$ (mV)	Non-normalized tail current $V_{0.5}$ (mV)	Slope (mV)
Control	-45.3 ± 2.4 (n =5)	-44.1 ± 3.9 (n =5)	6.8 ± 1.9 (n =5)
0.1 μM	-44.9 ± 1.2 (n =5)	-44.2 ± 3.1 (n =5)	7.5 ± 1.0 (n =5)
1 μM	-46.4 ± 1.2 (n =5)	-47.6 ± 4.8 (n =5)	7.4 ± 1.2 (n =5)
10 μM	-47.2 ± 0.9 (n =5)	-49.8 ± 6.3 (n =5)	7.6 ± 0.7 (n =5)
100 μM	-47.3 ± 0.9 (n =5)	-49.2 ± 5.1 (n =5)	7.4 ± 0.7 (n =5)
1 mM	-46.7 ± 0.9 (n =5)	-49.7 ± 5.8 (n =5)	7.4 ± 0.7 (n =5)

Table S15. Summary of effects of aloperine on KCNQ5-R212A channels.

Statistics versus same channel in absence of aloperine. Values indicate mean ± SEM.